IEEE Access
Multidisciplinary ⋮ Rapid Review ⋮ Open Access Journal

Received March 18, 2021, accepted March 29, 2021, date of publication April 1, 2021, date of current version April 14, 2021.

Digital Object Identifier 10.1109/ACCESS.2021.3070440

Stiffness Prediction and Analysis of Composite Leaf Springs

HELONG LIU[1], WENKU SHI[1], RUI GAO[2], ZHIYONG CHEN[1], AND HUANG CHEN[2]

[1]State Key Laboratory of Automotive Simulation and Control, Jilin University, Changchun 130022, China
[2]Automotive Research Institute, China National Heavy Duty Truck Group Company Ltd., Jinan 250100, China

Corresponding author: Wenku Shi (shiwk@jlu.edu.cn)

This work was supported in part by the National Key Research and Development Program of China under Grant 2018YFB0106200, in part by the Industrial Technology Research and Development Funds of Jilin Province under Grant 2019C041-4, and in part by the Key Scientific and Technological Research Projects of Jilin Province under Grant 20170204063GX.

ABSTRACT Composite leaf springs represent a key application of composite materials in the field of automotive lightweight materials. Stiffness, as a critical parameter of composite leaf springs, is closely related to the handling stability and ride comfort of automobiles. Therefore, this paper proposes an explicit theoretical model, which can consider the anisotropy of composite materials and detailed structure of the leaf spring, to predict the stiffness based on the law of energy conservation. The obtained results are verified against the results of the finite element method and bench test of basalt/epoxy samples. Moreover, the influence of the relevant design parameters on the stiffness is analyzed to provide guidance for the stiffness matching of composite leaf springs. The thickness of the composite leaf spring considerably influences its stiffness. As a key parameter representing the bearing capacity, the strength is closely related to the reliability of leaf springs. Based on the Tasi-Wu strength failure criterion, the influence of the relevant design parameters on the strength ratio of a composite leaf spring is analyzed under the constraint of stiffness. An increase in the width of the composite leaf spring enhances its bearing capacity when the stiffness is required to be within a certain range.

INDEX TERMS Automotive lightweight, composite leaf spring, stiffness prediction, finite element method, theoretical model.

I. INTRODUCTION

With the requirements pertaining to energy saving and environmental protection becoming increasingly stringent, automotive lightweight technology has received widespread attention [1]–[3]. Composite materials have demonstrated considerable potential to serve as automobile lightweight materials owing to their high specific strength/modulus and excellent fatigue performance [4]–[6]. In this regard, extensively examining the application of composite materials in the automobile domain is of significant engineering value.

As one of the mature automobile suspension structures, a leaf spring stores potential energy as strain energy through the spring deformation to absorb the energy of vertical vibrations, bump loads, and shocks, and gradually releases this energy [7]. Composite leaf springs represent a notable application of composite materials in the automobile lightweight domain [8]–[10]. In general, the weight of a leaf spring accounts for 10-20% of the unsprung weight [11]. Compared to traditional metal leaf springs, composite leaf springs not only reduce the total mass and improve the fuel economy, but also increase the driving safety and riding comfort [12]. Therefore, many researchers have focused on composite leaf springs in recent years [13]–[15].

With the continuous progress of the automobile industry, the importance of the research on the vehicle ride comfort is becoming increasingly prominent [16], [17]. The stiffness is a key basic performance parameter of a leaf spring, which is closely related to the handling stability and ride comfort of an automobile. The efficiency and accuracy of stiffness prediction determine the development cost of composite leaf springs. However, the inhomogeneity and anisotropy of composite materials render it highly complex and difficult to predict the stiffness of composite leaf springs [18].

At present, two main methods are available to calculate the stiffness of composite leaf springs, i.e., finite element method (FEM) and theoretical model method. As a relatively mature theory, the accuracy of FEM results is generally

The associate editor coordinating the review of this manuscript and approving it for publication was Xiaosong Hu.

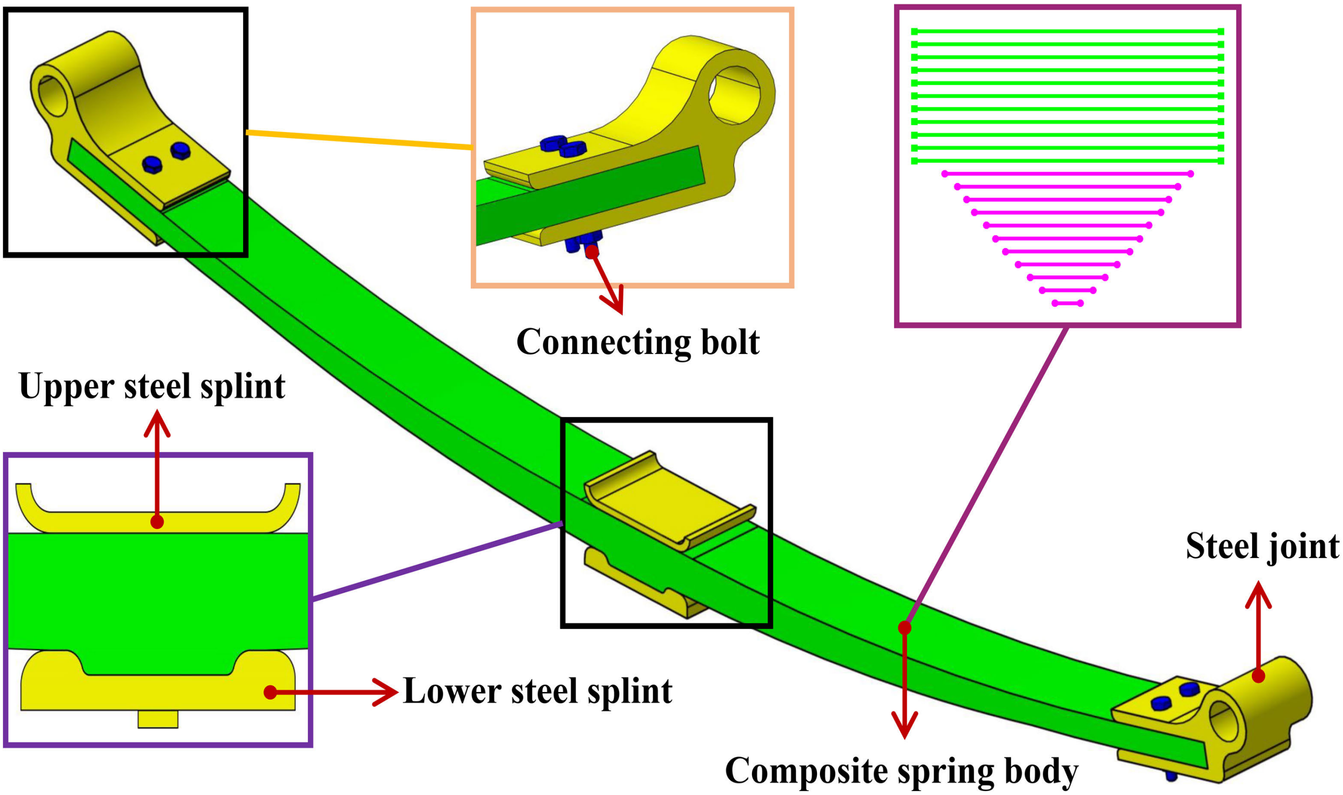

FIGURE 1. Structure of a composite leaf spring.

higher because the details of structure can be considered in the model. Wang *et al.* used the FEM to predict the stiffness and bearing capacity of a composite leaf spring for a commercial vehicle and verified the results via sample testing [19]. Kessentini *et al.* adopted the FEM to conduct the design and static analysis of a 3D-printed carbon polyether ether ketone polymer-based composite mono leaf spring [20]. However, the FEM application involves a large modeling and operation cycle, which hampers the design and optimization of composite leaf springs in the development stage. To compensate for these limitations, certain scholars attempted to establish theoretical models regarding the stiffness of composite leaf springs. Shokrieh *et al.* proposed a theoretical calculation method to predict the stiffness of composite leaf springs in the initial study stage [21]. However, the anisotropy of the composites and detailed structure of the leaf spring were not considered in this approach. Ke *et al.* established a theoretical model to predict the stiffness of composite leaf springs by employing the infinitesimal method, which was verified through the FEM and test results [22]. On this basis, Shi *et al.* considered the neutral layer displacement coefficient of the composite spring body in the theoretical model [23]. Yang *et al.* verified the effectiveness of the energy method to predict the stiffness of a composite leaf spring in the model [24]. However, these theoretical models to calculate the stiffness of composite leaf springs are generally based on the lamination scheme for integral calculation. During the forward design optimization of composite leaf springs, the ideal solution cannot be easily obtained if the length of each layer is considered as an optimization variable, as such as approach increases the cost and difficulty of development of the leaf springs.

Considering these aspects, in this study, an explicit theoretical model is developed to predict the stiffness of composite leaf springs based on the law of energy conservation. The key differences between the proposed model and the existing calculation methods can be summarized as follows:

(a) The anisotropy of composite materials and detailed structure of the composite leaf spring are considered in the proposed model; (b) an explicit formula to calculate the stiffness of composite leaf springs is adopted to enhance the stiffness calculation efficiency and shorten the development cycle of composite leaf springs. (c) starting from the shape of the spring body, the proposed model contains fewer design parameters, thereby facilitating the forward design and optimization of composite leaf springs.

Based on the theoretical model, the influence laws of the relevant design parameters on the stiffness of composite leaf springs are extensively analyzed. In addition, the strength characteristics of composite leaf springs are analyzed under the constraint of stiffness to provide a reference for the forward development of leaf springs.

II. STRUCTURE OF A COMPOSITE LEAF SPRING

The structure of a composite leaf spring is shown in Fig. 1.

The composite leaf spring assembly mainly consists of four parts: a composite spring body, two steel joints, an upper steel splint, and a lower steel splint. The composite spring body, with a constant width and parabolic thickness, is made from fiber-reinforced resin matrix composites. The constant width design facilitates the cutting and stacking of the composite fabrics in volume production [18]. The parabolic thickness design is in accordance with the "equal stress beam" characteristic, which can not only increase the utilization rate of materials and satisfy the lightweight requirements, but also increase the bearing capacity of a leaf spring when the stiffness is required to be within a certain range. The composite spring body is connected with the automotive frame through steel joints fixed by two connecting bolts. The upper and lower steel splints are fixed to the middle segment of the composite spring body through a high-strength adhesive to enable accurate positioning of the leaf spring assembly and avoid direct contact between the U-bolts of the suspension and composite spring body. In addition, the convex platform in the middle segment of the spring body operates in combination with the groove of the lower steel splint to ensure the reliable transmission of the longitudinal force between the spring body and lower steel splint. In contrast with the bolted structure, the convex structure can avoid the drilling of the middle segment of the composite spring body, which helps enhance the fatigue performance of the composite leaf spring.

III. THEORETICAL MODEL TO PREDICT THE STIFFNESS OF COMPOSITE LEAF SPRINGS

The main difference between fiber-reinforced composites and traditional metal materials is that the former and latter materials are considered to be anisotropic and isotropic, respectively. Therefore, the fiber ply direction must be considered in the design of the composite leaf spring body. In particular, a smaller number of fiber ply directions can help simplify the design and manufacturing work under the condition of meeting the design requirements. In addition, composite leaf springs must resist variable types of external loads dominated by vertical loads during their service life. Considering the fact that leaf springs are subjected to transverse loads (along the width direction, such as the turning condition of a car), herein, we consider the composite spring body to be composed of single layers arranged alternately in the $+\theta$ and $-\theta$ configurations (θ is the angle between the fiber ply direction and circumferential direction of the leaf spring).

A. CALCULATION OF OFF-AXIS ELASTIC PARAMETERS

When analyzing and designing fiber-reinforced composites, the single layer is usually assumed to be in a plane stress state. Thus, only the stress components in the plane are considered, and the interaction between the layers is ignored. The mechanical analysis of a single layer involves two elastic principal stress directions of the materials, specifically, the longitudinal (fiber direction) and transverse (perpendicular to the longitudinal direction) directions, which correspond to higher and lower elastic moduli, respectively. The first and second axes are defined as the on-axes of the material, and the corresponding coordinate system is defined as the on-axis coordinate system. When the coordinate system of the structure (x-y coordinate system) does not coincide with the on-axis coordinate system of the material, the x-axis and y-axis are defined as off-axes, and the corresponding coordinate system is defined as the off-axis coordinate system.

The off-axis elastic parameters of fiber-reinforced resin matrix composites can be calculated as follows:

$$
\begin{aligned}
&E_x = \frac{\sigma_x}{\varepsilon_x^{(x)}} = \frac{1}{\bar{S}_{11}}, \quad E_y = \frac{\sigma_y}{\varepsilon_y^{(y)}} = \frac{1}{\bar{S}_{22}}, \quad G_{xy} = \frac{\tau_{xy}}{\gamma_{xy}^{(xy)}} = \frac{1}{\bar{S}_{66}} \\
&\nu_x = \frac{-\varepsilon_y^{(x)}}{\varepsilon_x^{(x)}} = \frac{-\bar{S}_{21}}{\bar{S}_{11}}, \quad \nu_y = \frac{-\varepsilon_x^{(y)}}{\varepsilon_y^{(y)}} = \frac{-\bar{S}_{12}}{\bar{S}_{22}}, \\
&\eta_{xy,x} = \frac{\gamma_{xy}^{(x)}}{\varepsilon_x^{(x)}} = \frac{\bar{S}_{61}}{\bar{S}_{11}}, \quad \eta_{xy,y} = \frac{\gamma_{xy}^{(y)}}{\varepsilon_y^{(y)}} = \frac{\bar{S}_{62}}{\bar{S}_{22}}, \\
&\eta_{x,xy} = \frac{\varepsilon_x^{(xy)}}{\gamma_{xy}^{(xy)}} = \frac{\bar{S}_{16}}{\bar{S}_{66}}, \quad \eta_{y,xy} = \frac{\varepsilon_y^{(xy)}}{\gamma_{xy}^{(xy)}} = \frac{\bar{S}_{26}}{\bar{S}_{66}}
\end{aligned} \tag{1}
$$

where E_x and E_y are the elastic moduli in the x-axis and y-axis, respectively. G_{xy} is the in-plane off-axis shear modulus. ν_x and ν_y are the Poisson's coupling coefficients. $\eta_{x,xy}$ and $\eta_{y,xy}$ are the tensile-shear coupling coefficients. $\eta_{xy,x}$ and $\eta_{xy,y}$ are the shear-tensile coupling coefficients. σ_x and σ_y are the stresses in the x-axis and y-axis, respectively. τ_{xy} is the in-plane shear stress. $\varepsilon_x^{(x)}$ is the strain in the x-axis, induced by σ_x. $\varepsilon_x^{(y)}$ is the strain in the x-axis, induced by σ_y. ε_y is the strain in the y-axis. γ_{xy} is the in-plane shear strain. $\bar{S}$ is the off-axis flexibility matrix, which can be obtained as follows:

$$
\begin{aligned}
\bar{S}_{11} &= S_{11}m^4 + (2S_{12} + S_{66})m^2n^2 + S_{22}n^4 \\
\bar{S}_{22} &= S_{11}n^4 + (2S_{12} + S_{66})m^2n^2 + S_{22}m^4 \\
\bar{S}_{12} &= \bar{S}_{21} = S_{12}(m^4 + n^4) + (S_{11} + S_{22} - S_{66})m^2n^2 \\
\bar{S}_{66} &= S_{66}(m^4 + n^4) + 2(2S_{11} + 2S_{22} - 4S_{12} - S_{66})m^2n^2 \\
\bar{S}_{16} &= \bar{S}_{61} = (2S_{11} - 2S_{12} - S_{66})m^3n - (2S_{22} \\
&\quad - 2S_{12} - S_{66})mn^3 \\
\bar{S}_{26} &= \bar{S}_{62} = (2S_{11} - 2S_{12} - S_{66})mn^3 - (2S_{22} \\
&\quad - 2S_{12} - S_{66})m^3n
\end{aligned} \tag{2}
$$

where

$$
\begin{aligned}
&S_{11} = \frac{1}{E_1}, \quad S_{22} = \frac{1}{E_2}, \quad S_{66} = \frac{1}{G_{12}}, \quad S_{12} = -\frac{\nu_2}{E_2} \\
&S_{21} = -\frac{\nu_1}{E_1}, \quad S_{16} = S_{61} = S_{26} = S_{62} = 0 \\
&m = \sin\theta, \quad n = \cos\theta
\end{aligned} \tag{3}
$$

where E_1 and E_2 denote the on-axis elastic moduli, G_{12} is the in-plane on-axis shear modulus, ν_1 is the longitudinal Poisson's ratio, ν_2 is the transverse Poisson's ratio, and $\nu_1/E_1 = \nu_2/E_2$.

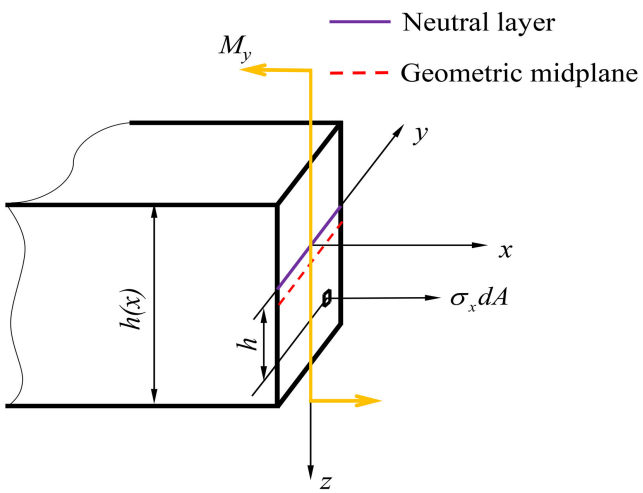

FIGURE 2. The cross-section element of the composite spring body.

B. CALCULATION OF THE BENDING RIGIDITY AT THE CROSS-SECTION

Due to the fact that the longitudinal dimension of the leaf spring is much larger than the thickness dimension and transverse dimension, the composite leaf spring can be simplified as Euler–Bernoulli beam [23]. Therefore, when analyzing the pure bending characteristics of the cross-section, only the longitudinal strain is considered, whereas other strains are ignored. The bending rigidity of the cross-section determines the vertical stiffness of the leaf spring. Many studies have demonstrated that the tensile elastic modulus and compressive elastic modulus of most materials, including several composites, are not equal [25]. The difference in the tensile modulus and compressive modulus may cause the offset of the neutral layer relative to the geometric midplane of the cross-section, which must be considered when calculating the bending rigidity of the cross-section.

An arbitrary cross-section element of the composite spring body with bending deformation was extracted, as shown in Fig. 2. Here, $h(x)$ is the thickness of the cross-section, M_y is the bending moment around the y-axis, σ_x is the stress along the x-axis at a certain position in the cross-section, h is the distance between a certain position and the neutral layer in the cross-section, and A is the area of the cross-section.

According to the research results of Jones [26], the position of the neutral layer of the unidirectional fiber laminates at the location x can be expressed as follows:

$$h_n^c(x) = \frac{\sqrt{E_x^t}}{\sqrt{E_x^t} + \sqrt{E_x^c}} h(x) \tag{4}$$

where $h_n^c(x)$ is the distance between the neutral layer and compressed side along the z-axis of the cross-section, E_x^t and E_x^c denote the off-axis tensile modulus and compressive modulus, respectively. Thus, the distance between the neutral layer and tensile side along the z-axis of the cross-section can be expressed as $h_n^t(x) = h(x) - h_n^c(x)$.

For the pure bending condition, the strain at a certain position of the bending cross-section is proportional to the distance from the neutral layer. Therefore, the stress at a certain position in the cross-section can be obtained using Hooke's law:

$$\sigma_x = E\varepsilon_x = Eh/\rho \tag{5}$$

where ε_x is the strain along the x-axis at a certain position, E is the elastic modulus at this position in the cross-section, and ρ is the curvature radius of the neutral layer.

The bending moment around the y-axis of the cross-section can be expressed as

$$\begin{aligned} M_y &= \int_A \sigma_x h dA \\ &= \int_{A^c} \frac{E_x^c h^2}{\rho} dA + \int_{A^t} \frac{E_x^t h^2}{\rho} dA \end{aligned} \tag{6}$$

where A^c and A^t denote the area of the compressed region and tensile region, respectively, and $A^c + A^t = A$.

According to Euler–Bernoulli beam theory, the width of the tensile region is equal to the width of the compressed region, and is equal to the width of the leaf spring. In addition, the bending radius ρ does not vary along the z-axis. Thus, the formula (6) can be converted to

$$\begin{aligned} M_y &= \int_{-h_n^c}^{0} \frac{bE_x^c h^2}{\rho} dh + \int_{0}^{h_n^t} \frac{bE_x^t h^2}{\rho} dh \\ &= \frac{b}{3\rho}\left[E_x^c (h_n^c)^3 + E_x^t (h_n^t)^3\right] \\ &= \frac{bh^3}{3\rho} \frac{E_x^t E_x^c}{(\sqrt{E_x^t} + \sqrt{E_x^c})^2} \end{aligned} \tag{7}$$

where b is the width of the composite leaf spring.

Therefore, the bending rigidity of the cross-section at location x can be expressed as

$$\begin{aligned} K(x) &= M_y(x)\rho(x) \\ &= \frac{bh(x)^3}{3}\xi \end{aligned} \tag{8}$$

where ξ is defined as the material coefficient indicated in (9).

$$\xi = \frac{E_x^t E_x^c}{(\sqrt{E_x^t} + \sqrt{E_x^c})^2} \tag{9}$$

According to (8), the bending rigidity of the cross-section is influenced by the material parameters, width of the composite leaf spring, and thickness of the cross-section.

C. THEORETICAL MODEL TO PREDICT THE STIFFNESS OF COMPOSITE LEAF SPRINGS

The front half of the leaf spring is considered as an example to calculate the stiffness. In the actual working process of the leaf spring, the middle segment of the leaf spring is connected to the axle of the automobile through the U-shaped bolts of the suspension, and the steel joints of the leaf spring are connected with the pin shafts of the frame. The vertical load on the wheel due to the road irregularities is transmitted to the

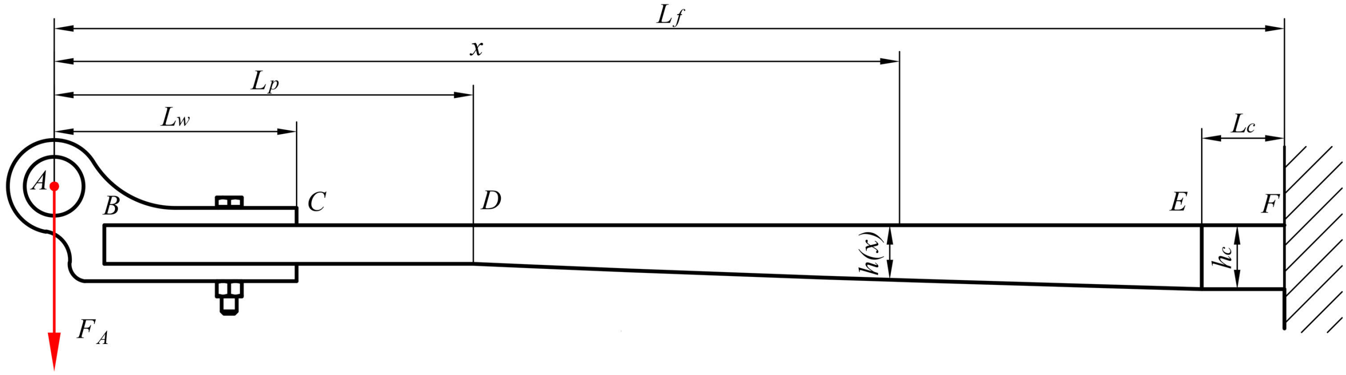

FIGURE 3. Structure and parameters of the front half of the composite leaf spring.

frame through the leaf spring. Thus, according to the actual loading state of the composite leaf spring, the front half of the leaf spring can be simplified as a cantilever structure. The middle segment of the leaf spring connected with the axle is the fixed end. The structure and related parameters of the front half of the composite leaf spring are shown in Fig. 3 (the convex platform in the middle segment of the composite spring body does not participate in the bending deformation, and thus, this particular platform is not shown in the figure). The width of the composite leaf spring is an arbitrary constant. Segment *BD* indicates the equal thickness of the composite body, in which segment *BC* is connected with the steel joint via connecting bolts. The elastic modulus of the resin matrix composite is considerably lower than that of steel, and thus, the bending deformation and rotation angle of segment *AC* can be ignored compared to those of segment *CE*. Segment *DE* is the variable thickness segment of the composite spring body, and the thickness variation follows the law of parabola. Segment *EF* clamped by the upper and lower steel splints is fixed on the axle through the U-shaped bolts, and thus, the bending deformation and rotation angle of segment *EF* can also be ignored compared with those of segment *CE*.

According to the law of parabola, the thickness variation in the composite spring body can be defined as in (10):

$$h(x) = \begin{cases} h_c(\dfrac{L_p}{L_f - L_c})^{1/2}, & x \leq L_p \\ h_c(\dfrac{x}{L_f - L_c})^{1/2}, & L_p < x \leq L_f - L_c \\ h_c, & L_f - L_c < x \leq L_f \end{cases} \tag{10}$$

When a vertical load F_A is applied to the end of the composite leaf spring, the bending moment of the cross-section at horizontal distance x is

$$M^{f,x} = F_A x \tag{11}$$

Thus, the bending strain energy of the cantilever beam can be calculated as

$$U = \int_0^{L_f} \frac{(M^{f,x})^2}{2K(x)} dx \tag{12}$$

Because segments *AC* and *EF* are regarded as non-bending deformation segments, the variation of the bending strain energy of the two segments is ignored. Therefore, (12) can be expressed as

$$U = \int_{L_w}^{L_p} \frac{(M^{f,x})^2}{2K(x)} dx + \int_{L_p}^{L_f - L_c} \frac{(M^{f,x})^2}{2K(x)} dx \tag{13}$$

According to (8)-(11) and (13), the bending strain energy can be expressed as follows:

$$U = \frac{F_A^2 \lambda}{2b\xi h_c^3} \tag{14}$$

where λ is the structure coefficient:

$$\lambda = 2(L_f - L_c)^3 - (\frac{L_f - L_c}{L_p})^{1.5}(L_P^3 + L_w^3) \tag{15}$$

The work done by F_A can be presented as

$$W = \frac{1}{2} F_A \delta \tag{16}$$

where δ is the vertical displacement caused by F_A.

According to the law of energy conservation, the strain energy of an elastic body is numerically equal to the work done by an external force, that is,

$$U = W \tag{17}$$

Therefore, the deflection of the front half of the leaf spring under F_A can be obtained:

$$\delta = \frac{F_A \lambda}{b\xi h_c^3} \tag{18}$$

When the structure of the composite leaf spring is asymmetrical, and the vertical load causing the same displacement at the end of the rear half of the composite leaf spring is F_r, the stiffness of the leaf spring assembly is

$$k = \frac{F_A + F_r}{\delta} \tag{19}$$

When the structure of the composite leaf spring is symmetrical, its stiffness is

$$k_s = \frac{2F_A}{\delta} = \frac{2b\xi h_c^3}{\lambda} \tag{20}$$

TABLE 1. Mechanical property parameters of Basalt/epoxy laminate.

Parameter	Value
Longitudinal tensile modulus E_1^t / MPa	40770
Longitudinal compressive modulus E_1^c / MPa	41710
Transverse tensile modulus E_2^t / MPa	10560
Transverse compressive modulus E_2^c / MPa	10120
In-plane shear modulus G_{12} / MPa	3330
Longitudinal tensile Poisson's ratio v_1^t	0.310
Longitudinal compressive Poisson's ratio v_1^c	0.317
Longitudinal tensile strength X_t / MPa	1150
Longitudinal compressive strength X_c / MPa	701
Transverse tensile strength Y_t / MPa	40
Transverse compressive strength Y_c / MPa	142
In-plane shear strength S_{12} / MPa	51

In summary, the stiffness can be predicted according to (1), (9), (15), and (18) to (20).

IV. VALIDATION OF THE THEORETICAL MODEL

A. MATERIAL SELECTION

The main function of the fiber-reinforcement in the composite is to bear the main load and provide the strength and stiffness. A fiber material is expected to have a high strength and stiffness, high corrosion resistance, and low density. As a continuous fiber drawn from natural basalt, basalt fiber, which exhibits excellent mechanical properties and can satisfy the requirements of leaf springs, is an inorganic green environmental protection material. Therefore, basalt fiber is selected as the reinforcement to manufacture the composite spring body in the following example. The main function of the matrix is to fix and protect the fibers and transfer the load among the fibers. The matrix material should not only form an excellent interface phase with the reinforcing fibers to ensure the composite has enough strength and toughness, but also exhibit a high infiltration, temperature resistance, corrosion resistance, and aging resistance [18]. The common matrices used in composite leaf springs are composed of epoxy resin and polyurethane. Epoxy resin pertains to convenient curing conditions and reasonable mechanical properties, and thus, epoxy resin is considered as the matrix material of the composite spring body. Furthermore, 40Cr steel is used to manufacture the other metal parts. The on-axis mechanical property parameters of basalt/epoxy laminate are listed in Table 1.

Leaf springs store and absorb the energy of vibration and shock in the form of strain energy. Therefore, the strain energy is a critical parameter of the material used to manufacture the composite spring body. The amount of elastic strain energy is proportional to the square of the allowable stress and inversely proportional to the modulus of elasticity in the circumferential direction of the leaf spring [27]. Moreover, fiber-reinforced resin matrix composites such as basalt/epoxy usually exhibit the highest energy storage properties in the fiber direction [21]. When the fiber direction of the composite is aligned with the circumferential direction of the composite leaf spring, the advantages of high modulus/strength of the fiber can be better utilized. Therefore, the fiber ply direction is selected to be aligned with the circumferential direction of the leaf spring in the following example.

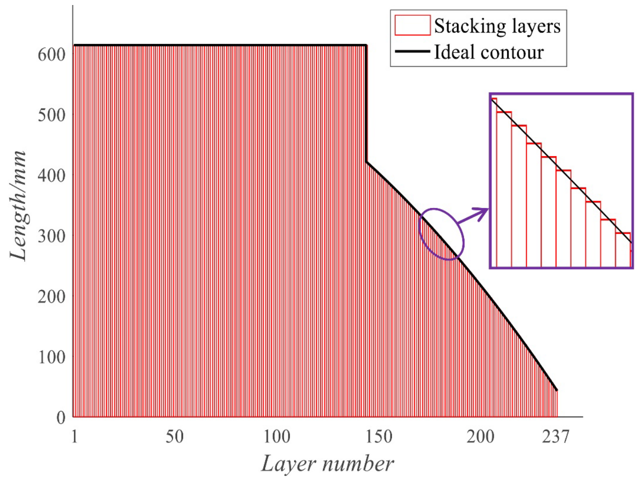

FIGURE 4. Comparison between actual stacking layers and ideal contour.

B. FEM AND THE BENCH TEST

The correctness of the theoretical model for the stiffness prediction of composite leaf springs is verified through the combination of FEM and bench testing. The leaf spring in the considered example is a front and rear symmetrical structure. The structural parameters of the composite leaf spring are listed in Table 2. The single-layer thickness of the basalt/epoxy composite laminates is 0.14 mm. The number of layers in the middle segment of the composite spring body is $n_c = 237$. The comparison between the actual stacking layers and ideal contour is shown in Fig. 4. The actual stacking layers are basically consistent with the designed parabolic contour.

The finite element analysis (FEA) model is established according to the actual stacking layers, as shown in Fig. 5. In the FEA model, a vertical load of 16500N is applied to the reference point coupled with the middle segment of the composite leaf spring. Points A and O are coupled with the center of the eye hole of the steel joint. Except for the movement along the x-axis and rotation along the y-axis, the other degrees of freedom of points A and O are restricted.

The samples of the composite leaf spring manufactured via the molding process are shown in Fig. 6. The stiffness test of the composite leaf spring is illustrated in Fig. 7. The middle segment of the composite leaf spring is clamped with the connecting steel block through the U-shaped bolts. The connecting block is connected with the actuator of the hydraulic machine PL63N. The steel joints of the leaf spring

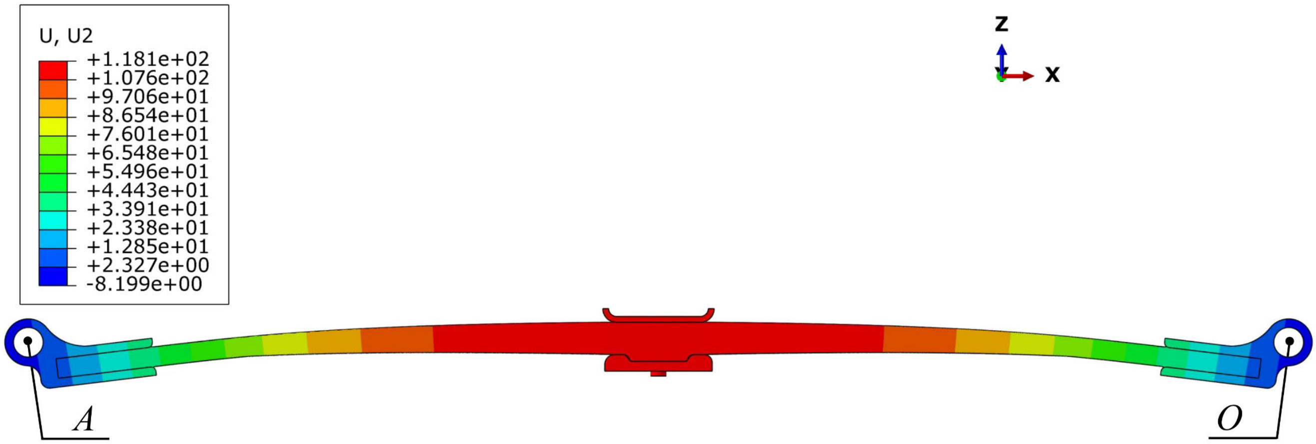

FIGURE 5. FEA model.

FIGURE 6. Samples of the composite leaf spring.

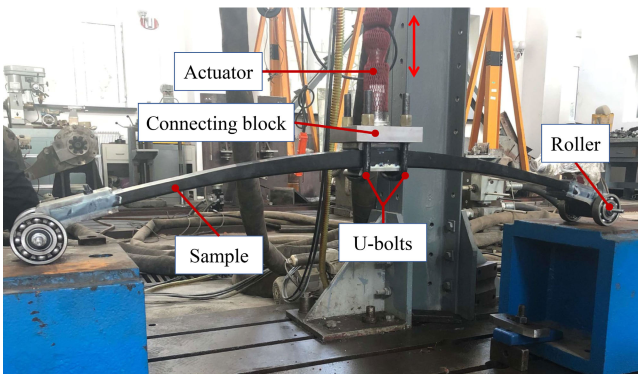

FIGURE 7. Stiffness test of the composite leaf spring.

TABLE 2. Structural parameters of the leaf spring.

Parameter	Value
Length of the front half L_f / mm	640
Length of the middle-clamped segment L_c / mm	43
Parabola starting length L_p / mm	218
Joint length L_w / mm	121
Thickness of the middle segment h_c / mm	33.18

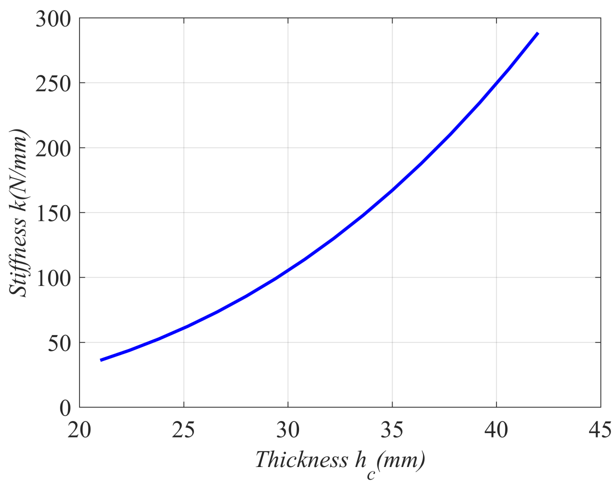

FIGURE 8. Influence law of the middle thickness (h_c) on the stiffness of the composite leaf spring.

are connected with the rollers to release the degree of freedom of movement and rotation. When the composite leaf spring is deformed under the vertical load, the roller can roll along the longitudinal direction of the leaf spring on the testbed. By controlling the actuator, the vertical load applied to the middle of the leaf spring is gradually increased from 0 to 16.5kN and then gradually removed. The force and corresponding displacement signals are extracted using the sensors in the actuator to obtain the stiffness test results of the composite leaf spring. The stiffness test results of the three samples shown in Fig. 6 are 142.06N/mm, 141.81N/mm, and 139.50N/mm. The mean stiffness is 141.1N/mm. The stiffness of the composite leaf springs predicted using the FEA and proposed approaches are compared with the test results, as presented in Table 3. The errors are less than 1% and can thus satisfy the requirements of engineering application.

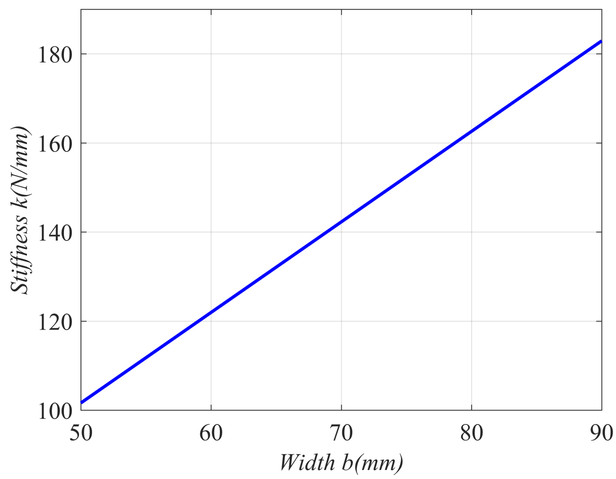

FIGURE 9. Influence law of the width (b) on the stiffness of the composite leaf spring.

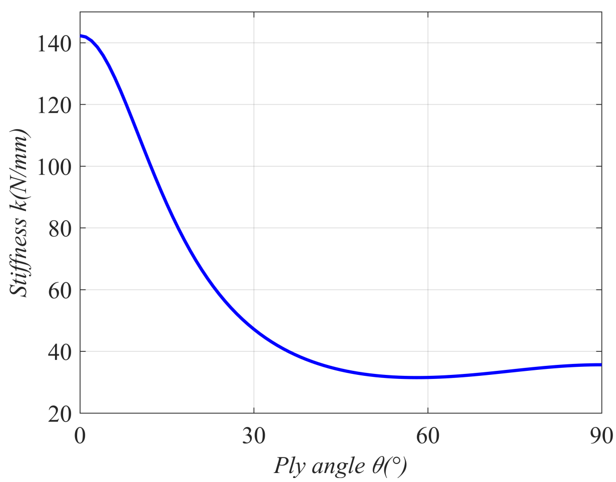

FIGURE 10. Influence law of the fiber ply angle (θ) on the stiffness of the composite leaf spring.

TABLE 3. Stiffness prediction results obtained using several approaches.

Approach	Stiffness/N·mm^{-1}	Error (%)
Test	141.1	\
FEA	139.7	0.99
Proposed model	142.27	0.83

The results show that the explicit theoretical model and FEA model to predict the stiffness of the composite leaf spring are correct and reliable.

V. INFLUENCE OF THE DESIGN PARAMETERS ON THE STIFFNESS

To provide guidance to realize the stiffness matching of composite leaf springs, the influence of the relevant design parameters on the stiffness is analyzed. When the materials used to manufacture the composite leaf spring are selected, the key design parameters include the number of layers (corresponding to the middle thickness of the composite spring body), width of the composite leaf spring, fiber ply angle, parabola starting length, and joint length. The influence law of each parameter on the stiffness of the composite leaf spring, derived by varying the corresponding design parameters in the model, is shown in Figs. 8-12.

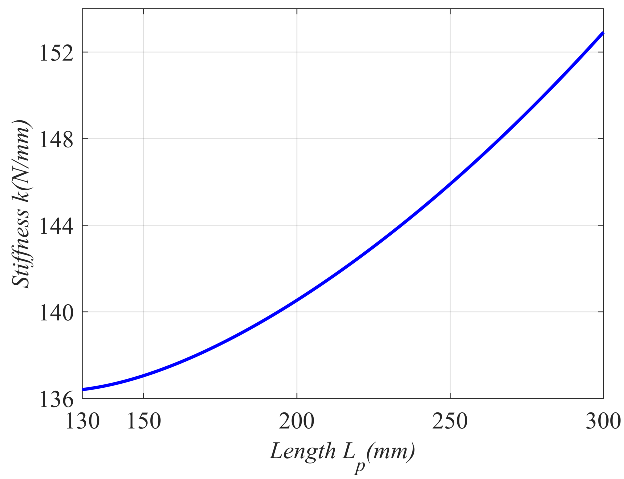

FIGURE 11. Influence law of the parabola starting length (L_p) on the stiffness of the composite leaf spring.

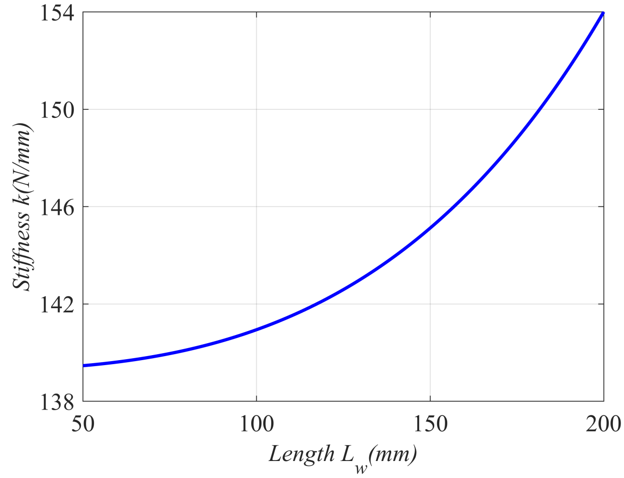

FIGURE 12. Influence law of the joint length (L_w) on the stiffness of the composite leaf spring.

The middle thickness of the composite spring body considerably influences the stiffness of the leaf spring, indicating that the number of layers can be changed to adjust the stiffness in a wide range. The width of the composite leaf spring is linearly correlated with the stiffness, and thus, the stiffness of the leaf spring can be adjusted linearly in a small range by changing the width of the leaf spring. The stiffness of the leaf spring is maximum and minimum when the fiber ply angle is equal to 0° and 40°-50°, respectively. In other words, the advantages of the high modulus of the fiber can be better utilized when $\theta = 0°$. The influence of the parabola starting length and joint length on the stiffness are small and nonlinear. Therefore, the stiffness can be adjusted in a small

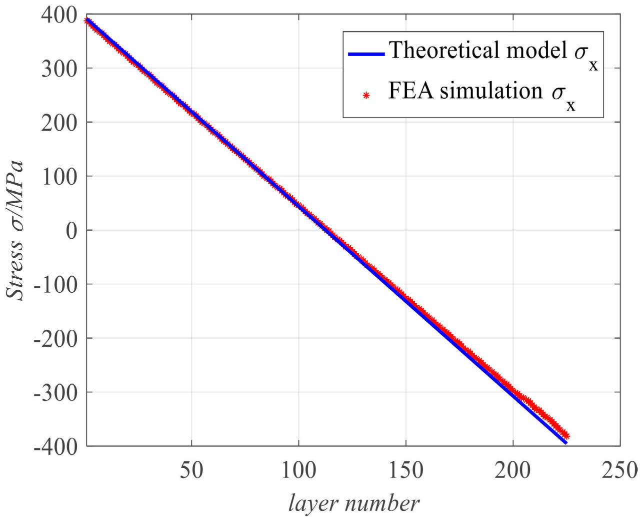

FIGURE 13. Comparison of the stress results obtained using the theoretical model and the FEA at 100 mm from center point F in the front half of the leaf spring.

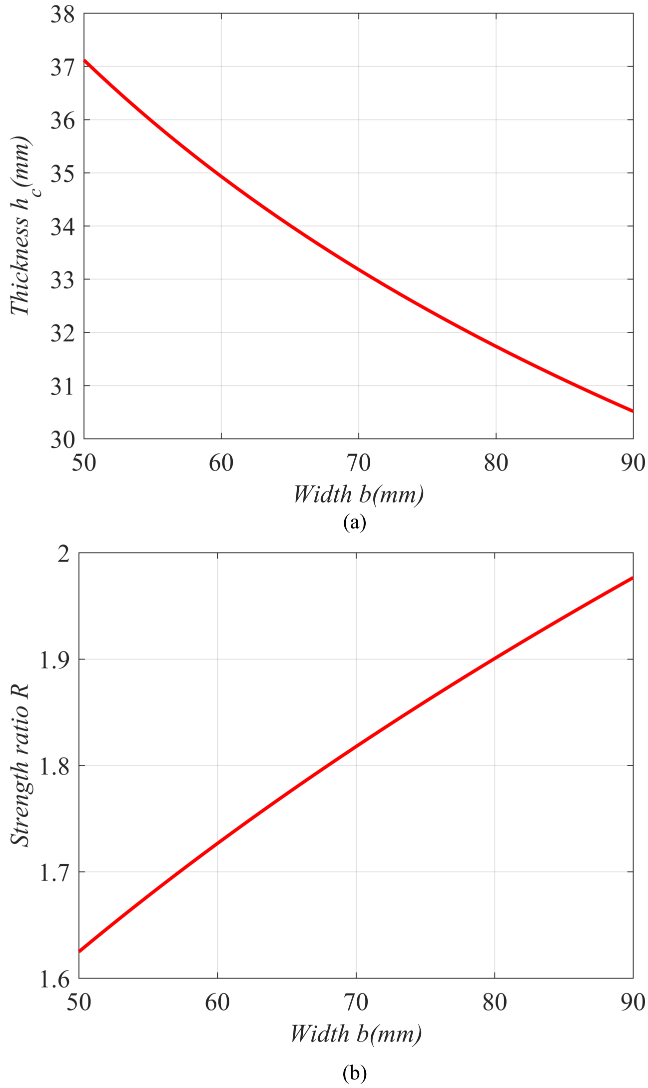

FIGURE 14. Variation in the (a) middle thickness of the leaf spring and (b) strength ratio with the width of the spring body.

range by changing the length of the two segments when the requirements for the connection strength between the end of the spring body and joint are satisfied.

VI. STRENGTH ANALYSIS OF THE COMPOSITE LEAF SPRING UNDER THE CONSTRAINT OF THE STIFFNESS

The main advantage of the parabolic thickness design is the "equal stress characteristic", according to which, segment DE exhibits approximately equal stresses, whereas segment AD exhibits a lower stress as the end part with equal thickness.

According to (5), the stress of each layer for any cross-section is proportional to the distance from the neutral layer along the z-direction. Therefore, the lowest strength of composite leaf spring assembly can be observed at the outer surface single layer of segment DE.

When the leaf spring is vertically bent, the upper and lower surfaces are subjected to tensile and compressive stresses, respectively. According to (4), (5), (8), (10), and (11), the off-axis longitudinal stress (circumferential direction) of the compressed outer surface single layer of segment DE can be calculated as

$$\begin{aligned}\sigma_x^c &= E_x^c \varepsilon_x^c \\ &= E_x^c \frac{h_n^c(x)M(x)}{K(x)} \\ &= \frac{3F_A(L_f - L_c)(\sqrt{E_x^t} + \sqrt{E_x^c})}{bh_c^2\sqrt{E_x^t}}\end{aligned} \tag{21}$$

The off-axis longitudinal stress of the tensile outer surface single layer of segment DE is:

$$\sigma_x^t = \frac{3F_A(L_f - L_c)(\sqrt{E_x^t} + \sqrt{E_x^c})}{bh_c^2\sqrt{E_x^c}} \tag{22}$$

The longitudinal stress results of the theoretical model and FEA simulation are shown in Fig. 13. The longitudinal stress of the numerical simulation is close to that of the FEA, which indicates that the conducted analysis based on the Euler-Bernoulli beam theory is reliable.

To evaluate the strength of the leaf spring, the concept of the strength ratio is introduced:

$$R = \frac{[\sigma_i]}{\sigma_i} \tag{23}$$

where σ_i is the applied stress component, and $[\sigma_i]$ is the ultimate stress component of the materials corresponding to σ_i. The physical meaning of strength ratio R is safety factor, and higher strength ratio corresponds to higher safety margin.

The Tasi-Wu strength failure criterion, which is widely used in the field of composite materials [28]–[30], is selected to examine the strength of the composite leaf springs. The single-layer strength ratio of composite materials can be

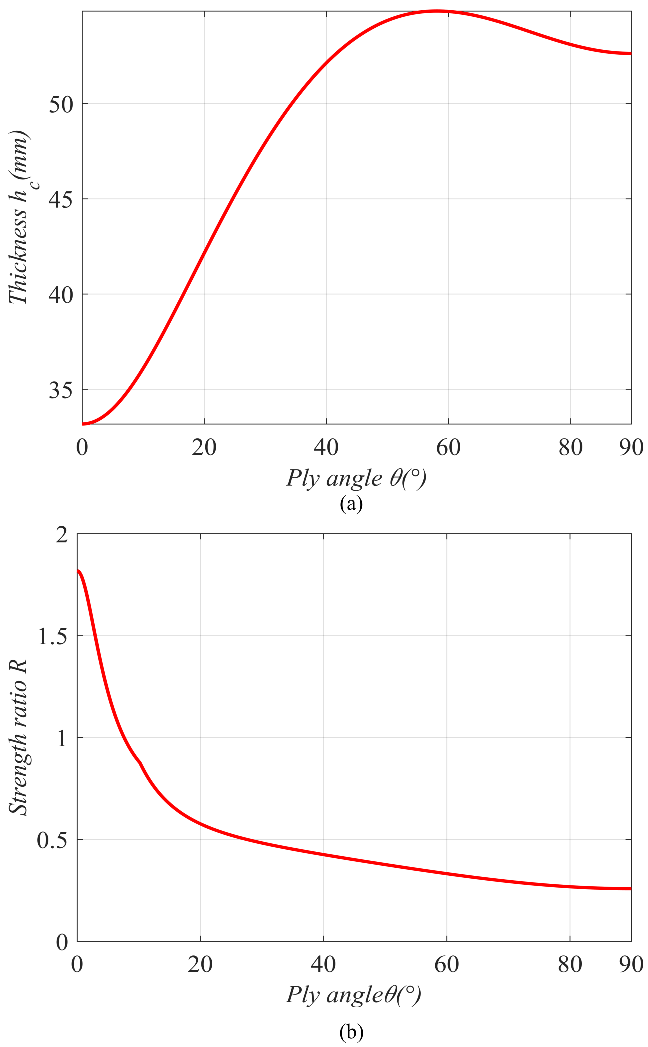

FIGURE 15. **Variation in the (a) middle thickness of the leaf spring and (b) strength ratio with the fiber ply angle.**

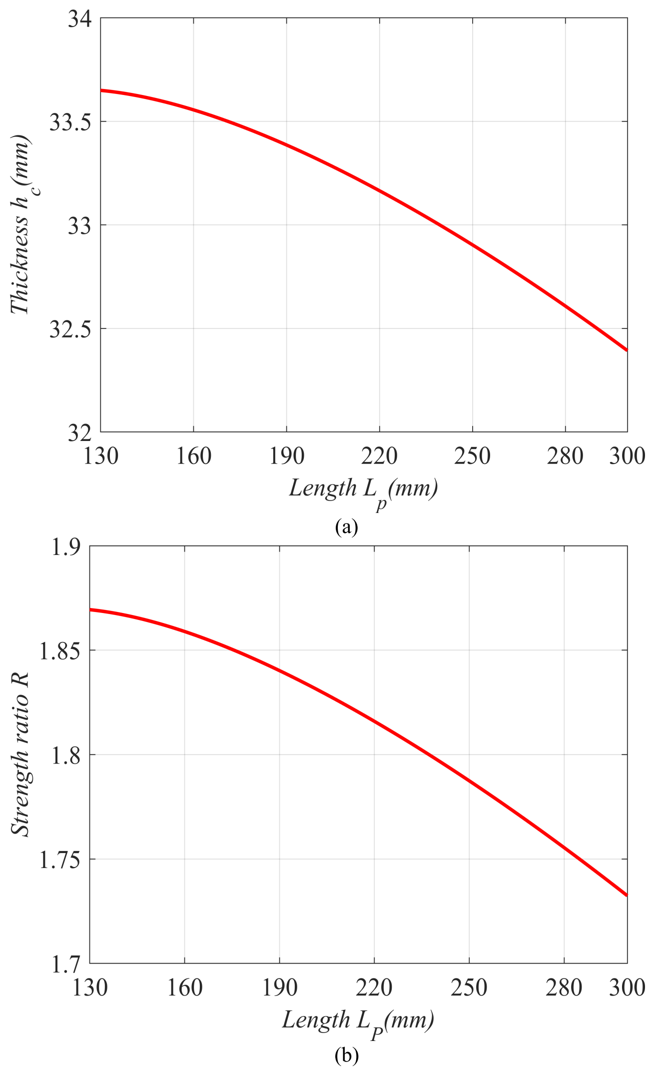

FIGURE 16. **Variation in the (a) middle thickness of the leaf spring and (b) strength ratio with the parabola starting length.**

calculated as follows:

$$(F_{11}\sigma_1^2 + 2F_{12}\sigma_1\sigma_2 + F_{22}\sigma_2^2 + F_{66}\tau_{12}^2) \times R^2 + (F_1\sigma_1 + F_2\sigma_2)R = 1 \quad (24)$$

where,

$$F_1 = \frac{1}{X_t} - \frac{1}{X_c}, \quad F_{11} = \frac{1}{X_t X_c}, \; F_2 = \frac{1}{Y_t} - \frac{1}{Y_c}$$
$$F_{22} = \frac{1}{Y_t Y_c}, \quad F_{66} = \frac{1}{S_{12}^2}, \; F_{12} = -\frac{1}{2}\sqrt{\frac{1}{X_t X_c Y_t Y_c}} \quad (25)$$

Under a certain load, the ultimate strength of a leaf spring with a larger stiffness is higher. However, the stiffness of the leaf spring is closely related to the handling stability and ride comfort of the automobile. Therefore, the stiffness of the composite leaf spring should first be matched reasonably, and then the strength design should be conducted under the constraint of the stiffness. According to (20)-(22), the middle thickness of the leaf spring considerably influences the stiffness and stress (higher power). Therefore, the influence of the relevant design parameters on the strength ratio of the leaf spring is analyzed by varying the middle thickness to control the stiffness of the leaf spring as a constant. The design parameters include the width of the composite leaf spring, fiber ply angle, parabola starting length, and joint length, as shown in Figs. 14-17.

When the stiffness is a constant, while the requirements of the assembly space are satisfied, increasing the width of the composite leaf spring can help increase the bearing capacity. The strength ratio is maximum when the fiber direction of the composite is the same as the circumferential direction of the leaf spring. In addition, when the fiber ply angle is 0°, a smaller middle thickness is beneficial to achieve a lightweight vehicle. The influence of the parabola starting length and joint length on the strength ratio of the leaf spring are small and nonlinear. Thus, while the requirements of the connection strength between the end of the spring body and

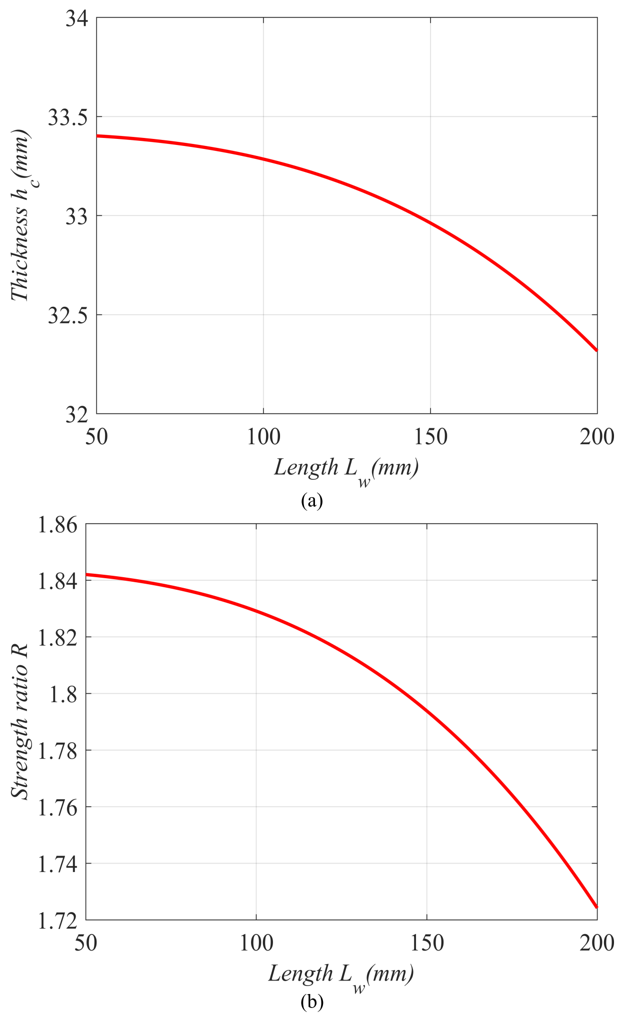

FIGURE 17. Variation in the (a) middle thickness of the leaf spring and (b) strength ratio with the joint length.

joints are satisfied, a smaller length of the two segments corresponds to a higher strength ratio.

VII. CONCLUSION

This paper proposes an explicit model to predict the stiffness of composite leaf springs, based on the law of energy conservation. The influence of the relevant design parameters on the stiffness is analyzed to provide guidance to realize the stiffness matching of composite leaf springs. Moreover, based on the explicit model, the influence of the relevant parameters on the strength ratio is examined to provide a reference for the forward development of leaf springs. The following key conclusions can be derived:

1. In contrast to the FEA, the theoretical model provides an explicit formula to predict the stiffness of the leaf spring, which can significantly enhance the calculation efficiency and shorten the development cycle of the leaf spring.

2. The middle thickness of the composite leaf spring is the design parameter that most notably influences the stiffness; moreover, the linear adjustment of the stiffness in a small range can be realized by changing the width of the leaf spring.

3. The increase in the width of the composite leaf spring can help enhance its bearing capacity when the stiffness is required to be within a certain range.

4. When the fiber ply direction is the same as the circumferential direction of the leaf spring, the optimal lightweight effect and bearing capacity of the composite leaf spring can be achieved.

In subsequent research, the design of the composite leaf spring must be further optimized to obtain the optimal structure and laminate scheme based on the proposed explicit stiffness model. In addition, the theoretical model should be further enhanced to consider external factors such as the driving state of the automobile.

REFERENCES

[1] J.-M. Lee, B.-J. Min, J.-H. Park, D.-H. Kim, B.-M. Kim, and D.-C. Ko, "Design of lightweight CFRP automotive part as an alternative for steel part by thickness and lay-up optimization," *Materials*, vol. 12, no. 14, p. 2309, Jul. 2019.

[2] Y. Pu, F. Ma, J. Zhang, and M. Yang, "Optimal lightweight material selection for automobile applications considering multi-perspective indices," *IEEE Access*, vol. 6, pp. 8591–8598, 2018.

[3] C. Jun, Z. Song-Lin, F. Jin-Zhi, and L. Xin-Tian, "A model of cumulative fatigue strengthening effect due to coaxing: Cumulative fatigue model," *Fatigue Fract. Eng. Mater. Struct.*, vol. 35, no. 5, pp. 433–440, May 2012.

[4] T. Heggemann and W. Homberg, "Deep drawing of fiber metal laminates for automotive lightweight structures," *Compos. Struct.*, vol. 216, pp. 53–57, May 2019.

[5] D. Rajak, D. Pagar, P. Menezes, and E. Linul, "Fiber-reinforced polymer composites: Manufacturing, properties, and applications," *Polymers*, vol. 11, no. 10, p. 1667, Oct. 2019.

[6] G. B. V. Kumar, R. Mageshvar, R. Rejath, S. Karthik, R. Pramod, and C. S. P. Rao, "Characterization of glass fiber bituminous coal tar reinforced polymer matrix composites for high performance applications," *Compos. B, Eng.*, vol. 175, Oct. 2019, Art. no. 107156.

[7] J. Jancirani and H. Assarudeen, "A review on structural analysis and experimental investigation of fiber reinforced composite leaf spring," *J. Reinforced Plastics Compos.*, vol. 34, no. 2, pp. 95–100, Jan. 2015.

[8] A. N. Polilov, N. A. Tatus, and X. Tian, "Analysis of efficiency of uniform-strength composite leaf springs under various loading conditions," *J. Machinery Manuf. Rel.*, vol. 48, no. 5, pp. 431–439, Sep. 2019.

[9] T. K. Vasan, S. M. Shibi, and C. K. Tamilselvan, "Fabrication and testing of composite leaf spring using carbon, glass and aramid fiber," *Mater. Today*, vol. 21, pp. 45–51, Jan. 2020.

[10] V. Khatkar and B. K. Behera, "Experimental investigation of composite leaf spring reinforced with various fiber architecture," *Adv. Compos. Mater.*, vol. 29, no. 2, pp. 129–145, Mar. 2020.

[11] K. Tanabe, T. Seino, and Y. Kajio, "Characteristics of carbon/glass fiber reinforced plastic leaf spring," *SAE Trans.*, vol. 91, pp. 1628–1636, Feb. 1982.

[12] I. Rajendran and S. Vijayarangan, "Optimal design of a composite leaf spring using genetic algorithms," *Comput. Struct.*, vol. 79, no. 11, pp. 1121–1129, Apr. 2001.

[13] D. Zindani, S. R. Maity, and S. Bhowmik, "Excogitating material rankings using novel aggregation multiplicative rule (AMR): A case for material selection problems," *Arabian J. Sci. Eng.*, vol. 45, no. 7, pp. 5631–5646, Jul. 2020.

[14] V. Khatkar, B. K. Behera, and R. N. Manjunath, "Textile structural composites for automotive leaf spring application," *Compos. B, Eng.*, vol. 182, Feb. 2020, Art. no. 107662.

[15] S. Rajesh, G. B. Bhaskar, J. Venkatachalam, K. Pazhanivel, and S. Sagadevan, "Performance of leaf springs made of composite material subjected to low frequency impact loading," *J. Mech. Sci. Technol.*, vol. 30, no. 9, pp. 4291–4298, Sep. 2016.

[16] X. Tang, X. Hu, W. Yang, and H. Yu, "Novel torsional vibration modeling and assessment of a power-split hybrid electric vehicle equipped with a dual-mass flywheel," *IEEE Trans. Veh. Technol.*, vol. 67, no. 3, pp. 1990–2000, Mar. 2018.

[17] Y. Qin, X. Tang, T. Jia, Z. Duan, J. Zhang, Y. Li, and L. Zheng, ''Noise and vibration suppression in hybrid electric vehicles: State of the art and challenges,'' *Renew. Sustain. Energy Rev.*, vol. 124, May 2020, Art. no. 109782.

[18] J. Ke, Z.-Y. Wu, X.-Y. Chen, and Z.-P. Ying, ''A review on material selection, design method and performance investigation of composite leaf springs,'' *Compos. Struct.*, vol. 226, Oct. 2019, Art. no. 111277.

[19] J. Wang, Z. Li, and Q. Jiang, ''The analysis of composite leaf spring by finite element method and experimental measurements,'' in *Proc. FISITA World Automot. Congr.*, vol. 195, SAE-China and FISITA, Eds. Berlin, Germany: Springer, 2013, pp. 823–829.

[20] A. Kessentini, G. M. S. Ahmed, and J. Madiouli, ''Design optimization and FE analysis of 3D printed carbon PEEK based mono leaf spring,'' *Micromachines*, vol. 10, no. 5, p. 279, Apr. 2019.

[21] M. M. Shokrieh and D. Rezaei, ''Analysis and optimization of a composite leaf spring,'' *Compos. Struct.*, vol. 60, no. 3, pp. 317–325, May 2003.

[22] J. Ke, W.-K. Shi, C. Qian, G.-M. Li, and K. Yuan, ''Prediction and matching design method for stiffness of composite leaf spring,'' *J. Zhejiang Univ., Eng. Sci.*, vol. 49, no. 11, pp. 2103–2110, Nov. 2015.

[23] W. Shi, C. Qian, Z. Chen, Q. Song, and S. Yang, ''Establishment of theoretical model of composite leaf springs by using the mechanics of composite materials,'' *J. Reinforced Plastics Compos.*, vol. 36, no. 18, pp. 1316–1326, Sep. 2017.

[24] S. Yang, W. Shi, Z. Chen, C. Qian, C. Yang, and L. Hang, ''Composite mechanics and energy method based stiffness prediction model for composite leaf springs,'' *Mech. Based Des. Struct. Mach.*, vol. 47, no. 3, pp. 375–386, May 2019.

[25] X.-T. He, Q. Chen, J.-Y. Sun, Z.-L. Zheng, and S.-L. Chen, ''Application of the kirchhoff hypothesis to bending thin plates with different Moduli in tension and compression,'' *J. Mech. Mater. Struct.*, vol. 5, no. 5, pp. 755–769, Dec. 2010.

[26] R. M. Jones, ''Apparent flexural modulus and strength of multimodulus materials,'' *J. Compos. Mater.*, vol. 10, no. 4, pp. 342–354, Oct. 1976.

[27] A. Corvi, ''A preliminary approach to composite beam design using FEM analysis,'' *Compos. Struct.*, vol. 16, nos. 1–3, pp. 259–275, Jan. 1990.

[28] L. Wan, Y. Ismail, C. Zhu, P. Zhu, Y. Sheng, J. Liu, and D. Yang, ''Computational micromechanics-based prediction of the failure of unidirectional composite lamina subjected to transverse and in-plane shear stress states,'' *J. Compos. Mater.*, vol. 54, no. 24, pp. 3637–3654, Oct. 2020.

[29] K. Yamaguchi, S. E. Phenisee, Z. Chen, M. Salviato, and J. Yang, ''Ply-drop design of non-conventional laminated composites using Bayesian optimization,'' *Compos. A, Appl. Sci. Manuf.*, vol. 139, Dec. 2020, Art. no. 106136.

[30] M. Imran, D. Shi, L. Tong, H. M. Waqas, R. Muhammad, M. Uddin, and A. Khan, ''Design optimization and non-linear buckling analysis of spherical composite submersible pressure hull,'' *Materials*, vol. 13, no. 11, p. 2439, May 2020.

HELONG LIU was born in Changchun, Jilin, China, in 1995. He received the B.S. degree from Jilin University, China, in 2017, where he is currently pursuing the Ph.D. degree with the College of Automotive Engineering. His research interests include automotive systems dynamics and structural designing of composites.

WENKU SHI received the Ph.D. degree from Jilin University, China, in 1996. He is currently a Professor with the College of Automotive Engineering, Jilin University. His research interests include automotive NVH and automotive lightweight techniques.

RUI GAO is currently the Manager of the China National Heavy Duty Truck Engineering Technology Research Center. His research interests include advanced air suspension systems, leaf spring suspension systems, and automotive lightweight techniques.

ZHIYONG CHEN received the Ph.D. degree from Jilin University, China, in 2011. He is currently an Associate Professor with the College of Automotive Engineering, Jilin University. His research interests include CAE, automotive lightweight techniques, and automotive NVH.

HUANG CHEN received the M.S. degree from Tsinghua University, China, in 2018. He is currently an Engineer with the China National Heavy Duty Truck Engineering Technology Research Center. His research interests include advanced components development of heavy-duty truck and automotive lightweight techniques.